Available online at www.sciencedirect.com
SCIENCE DIRECT®
Journal of Power Sources 145 (2005) 463–469
JOURNAL OF POWER SOURCES
www.elsevier.com/locate/jpowsour

Steady state and transient thermal stress analysis in planar solid oxide fuel cells

Azra Selimovic *, Miriam Kemm, Tord Torisson, Mohsen Assadi

Department of Heat and Power Engineering, Lund University, PO Box 118, S-221 00 Lund, Sweden

Accepted 24 November 2004
Available online 29 April 2005

Abstract

Resulting from elevated temperatures the major structural problem foreseen with planar SOFCs is their thermal stress. Due to the brittle nature of ceramic material, operation in or near the material plastic limit can be very critical. Therefore stress levels must always be kept below the tensile and shear limits. The analysis is focused on determination of the stress caused by the difference in thermal expansion coefficients when high temperature gradients occur in the SOFC layers during steady state and transient operation (heat-up, start-up and shut-down). Utilizing an in-house developed tool for assessment of the electrochemical and thermal performance of a bipolar planar cell the input temperature profiles are generated for a finite element analysis code to predict thermal component of the stress. The failure criterion adopted is based on the strength of the cell materials and the principal stresses developed by the thermal loading. To visualize the stress concentration in the fuel cell layers, maximum principal stress is calculated and compared with the yield strength of the SOFC materials found in the literature. The in-house code is capable to predict both steady state and dynamic temperature profiles. Of particular importance is the knowledge gained of the transient stress in the cell, which can be used to establish control parameters during transient operations.

Keywords: Solid oxide fuel cell; Fuel cell modelling; Thermal stress; Transient analysis

1. Introduction

Solid oxide fuel cell (SOFC) has been identified as a forward-looking technology for a highly efficient, environmentally friendly power generation. Within recent years substantial progress in materials and fabrication-technologies enabled both prototype and field tests of SOFC-systems for small stationary applications in the power range of 1–200 kW capable of electrical net efficiencies between 48 and 52% (in stand alone and hybrid concepts, respectively). Regarding the fuel cell electrical performance future SOFC systems for stationary applications are targeting power densities larger than 0.25 W cm^{-2} with degradation rates lower than 1 $\mu V\ h^{-1}$ and fuel utilization larger than 80% [1]. Target SOFC lifetimes are of the order 10^4 to 10^5 h [2].

Recognizing advantages of the low-cost and high volume manufacturing with high volumetric power densities, most of the fuel cells manufacturers are concentrating on the planar SOFC concept. However, a challenge with the planar geometries is in obtaining mechanically stable structure, as thin layer ceramics are inherently susceptible to failure when subjected to moderate stresses. The developers have found that when scaling up planar cells much beyond 100 cm^2 active area they become prone to mechanical failure [3]. The stresses to which the ceramic components are subjected can arise from: manufacturing (residual stresses); differential thermal expansion coefficients (TEC) of the cell layers; spatial or temporal temperature gradients; oxygen activity gradients; and external mechanical loading. The magnitude of the stresses depends on the materials properties, the operating conditions and the geometry of the design [4]. Residual stresses will arise from the difference between the thermal expansion coefficients and the effective Young's modulus of adjacent layers. These mismatch stresses can result in delam-

* Corresponding author. Tel.: +46 462229231; fax: +46 462224717.
E-mail address: azra.selimovic@vok.lth.se (A. Selimovic).

0378-7753/$ – see front matter © 2005 Elsevier B.V. All rights reserved.
doi:10.1016/j.jpowsour.2004.11.073

ination of layers or formation of micro-cracks in the weaker layers [5]. Stresses caused by the thermal gradients and thermal expansion mismatches will increase with increasing cell area which conflicts with the desire to maximize the active cell area and therefore output. Further, SOFC stacks are mechanically loaded with weights, during operation, in order to secure proper alignment and good contact between the cell components. This, together with the seals required around the edges of cells to separate the fuel and air compartments, can cause higher mechanical stresses transmitted to brittle elements in the stacks.

Practical applications for fuel cell systems are obviously the best way of testing the viability of a particular system. Nevertheless, for advancing the understanding of the fuel cell systems, computational models can be very useful. In the literature, there is a plethora of mathematical models describing general thermal–electrical planar SOFC performance [6–12]. However very few of them [9] are capable of simulating dynamic fuel cell behavior with more than one spatial dimension and most of the authors do not consider the thermal stress modeling with exception of [12].

The aim of this work was to develop a fuel cell modeling tool which couples thermal and structural analysis to provide not only the information about the cell's electrical performance but also to give further insight to the cell's structural response to different choices of the design parameters and also to different operating conditions. For a system designer this will allow to define safe operational points for the component while optimizing the system performance. Especially, the thermal stresses caused by spatial and temporal temperature gradients and mismatches in TEC between the different cell layers are under study. After the model development parametric analysis has been performed to identify some of the design parameters and operating conditions which may be important for the structural reliability of the fuel cell system.

2. SOFC modeling

2.1. Steady state model

A 2D model, based on the finite volume method, has been developed in FORTRAN for simulation of a planar electrolyte supported SOFC with internal reforming and bipolar interconnect (IC) plates. The model was described in depth in [13]. The investigated cell geometry is shown in Fig. 1 together with a characteristic volume element. The model allows for calculation of the temperature and current density distribution, the species concentration, and the channel flows. This requires solution of mass balances of the chemical species and the energy balances of the gases in the gas channels and the energy balance in the solid structure for each volume element.

The steady state model was validated by comparison of the simulated results to the results of different models from literature obtained for two benchmark tests. Standard benchmark tests were defined for a flat plate SOFC design and the test input conditions have been set up according to IEA Annex II report [14]. The developed model showed good agreement with the other model results and it has been accepted as a reliable tool for fuel cell performance simulation [13].

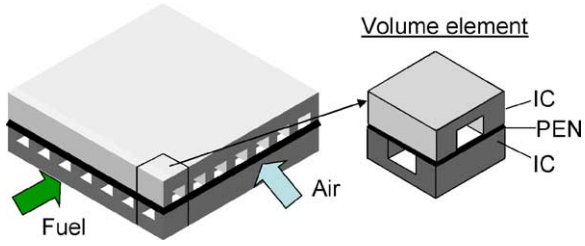

Fig. 1. Investigated cell design.

2.2. Dynamic modeling

For the investigation of unsteady processes the 2D, steady state, fuel cell model has been completed to allow for dynamic analysis. Looking at the transients of the transport phenomena taking place within the SOFC, electrochemical and electrical changes occur very fast in comparison to thermal changes [15]. Further the relaxation time for convective heat transfer is about a millisecond while conduction takes several seconds to relax. Thus, the major assumption of the dynamic model is that the transient term needs to be included only in the energy balance of the solid material of the cell and it is given by the left hand side of Eq. (1):

$$V\rho C_{\mathrm{p}}\frac{\partial T_{\mathrm{s}}}{\partial t} = \lambda_x\frac{\partial^2 T_{\mathrm{s}}}{\partial x^2} + \lambda_y\frac{\partial^2 T_{\mathrm{s}}}{\partial y^2} + \sum_{\mathrm{gas}} A_{\mathrm{gas}}\alpha_{\mathrm{gas}}(T_{\mathrm{s}} - T_{\mathrm{gas}}) + Q \quad (1)$$

where V represents the volume of the characteristic element, ρ and C_{p} represent specific density and specific heat of the solid material respectively. To enable simulations of transient heat up and shut-down, chemical reactions can be excluded from the model.

Due to lack of the experimental data for transient model validation a qualitative comparison has been made to a model from the literature [9] and shown good agreement.

2.3. Structural mechanics model

Thermal stress in the three-layered structure (anode, electrolyte and cathode) was calculated using the solid model within Structural Mechanics Module in the commercial finite element based tool FEMLAB [16]. With the electrochemical–thermal FORTRAN code, first the temperature field in the fuel cell is solved. In-plane temperature gradients are calculated in an intermediate step and imported to the FEA code. It has been assumed that the same temperature field occurs in each of the fuel cell layers i.e. the in-plane

Table 1
Material data for the fuel cell materials

Material	Young modulus (GPa)	Poisson's ratio	Thermal expansion coefficient (K^{-1})	Mechanical strength (MPa)
8YSZ	215 [2]	0.32 [2]	10e-6	14.1 at $W = 10^{-6}$, 30 at $W = 10^{-5}$ [17]
LSM	35 [2]	0.25 [2]	11e-6	6.6 at $W = 10^{-6}$, 9.3 at $W = 10^{-5}$ [17]
Ni-YSZ	55 [2]	0.17 [2]	13e-6	58 at $W = 10^{-6}$, 71 at $W = 10^{-5}$ [17]

temperature gradients are much larger than cross-plane gradients (through the cell thickness). Although the model solves only for mechanical stresses in the three-layered structure, the impact of the interconnect layers is accounted for in the heat balance of the solid, and in the ohmic resistance term of the electrochemical–thermal model. An unconstrained cell plate has been assumed and the analysis is fully elastic.

The typical materials used in the state-of-the-art fuel cells and also assumed for this study are as follows: (1) cathode – Sr doped $LaMnO_3$ (LSM), (2) electrolyte – Y_2O_3-doped ZrO_2 (YSZ), and (3) anode – Ni + YSZ. In Table 1 the Young's moduli, the thermal expansion coefficient, and the Poisson's ratio of the cell materials used in the study are given. All of the materials were assumed to be isotropic.

The calculated stresses are compared to the mechanical strength of the cell materials, which is also given in Table 1 and was taken from the work of Montros et al. [17] who used Weibull statistics to describe ceramic failure behavior of laminated SOFC plates. Since the analysis in [17] was purely theoretical, an experimental confirmation of the results is necessary.

3. Investigated cases

The base case for both steady-state and transient calculations is a thick electrolyte cell with ceramic interconnect and a mean operating temperature of 950 °C fuelled with 30% pre-reformed natural gas and with gases arranged in cross-flow. The fuel cell operates under uniform mass flow distribution of the feed gases with fuel utilization of 85% and average current density of 0.3 A cm^{-2}. The fuel flow is chosen to meet the required fuel utilization and the air flow is adjusted to limit the maximum solid temperature to 1050 °C. The following cases are investigated for steady state stress analysis, all with different configurations of the gas flows:

- Hydrogen-fuelled cell with ceramic interconnect.
- Hydrogen-fuelled cell with metallic interconnect.
- Methane-fuelled cell with ceramic interconnect.
- Methane-fuelled cell with metallic interconnect.

To describe the performance of the cell with metallic interconnect it has been assumed that the structure is still electrolyte-supported and that only ceramic interconnect material has been replaced with metallic material without changes of the cell geometry (i.e. layer thicknesses). In the case of the hydrogen-fuelled cell the fuel consists of a hydrogen and water vapor mixture (90% H_2, 10% H_2O). Coefficients for heat conduction for the different materials are set to 2 and 49 W m^{-1} K^{-1} [18] for ceramic and metallic interconnect respectively. The cell with metallic interconnect is operated at a cell voltage of 0.7 V while the voltage was set to 0.73 V for the cell with metallic interconnect.

The problem of thermal expansion mismatch in the present SOFCs mainly centers on the anode, since nickel has a higher coefficient of thermal expansion than YSZ. The anodes typically must contain more than 30 vol.% nickel to have sufficient conductivity [19]. A parametric study has been performed with variable expansion coefficients of the anode and cathode to study the impact on the thermal stress of these design parameters.

For transient SOFC simulations the following operation modes were defined:

- *Heat-up*: To enable start of the electrochemical reactions within the SOFC, the cell has to be heated up from ambient temperature to start-up temperature (700 °C). For heat-up simulations, an air stream with a mole flow rate of 10.6 mol h^{-1} was fed into the air channels. This airflow corresponds to the amount of air needed to fulfill the operating conditions described for the base case when applying ceramic IC. The difference between the minimum temperature of the cell and the temperature of the incoming air was held constant as shown in Eq. (2):

$$T_{\text{air,in}} = T_{\text{solid,min}} + \Delta T \quad (2)$$

- *Start-up*: When the heat-up process is finished the temperature level necessary for starting the electrochemical reactions is reached. Air and fuel of 900 °C are fed into the cell. The fuel flow is chosen to meet the required fuel utilization and the air flow is adjusted to limit the maximum solid temperature to 1050 °C.
- *Shut-down*: When starting the shut-down process, the current density and the inlet fuel mass flow are set equal to zero. Afterwards, the SOFC is cooled down to ambient temperature by feeding a cold air stream of 10.6 mol h^{-1} into the air channels. The inlet air temperature is controlled by Eq. (3):

$$T_{\text{air,in}} = T_{\text{solid,max}} - \Delta T \quad (3)$$

4. Model results

4.1. Steady state results

Fig. 2 shows an example of the output from the electrochemical–thermal model and from the stress model for

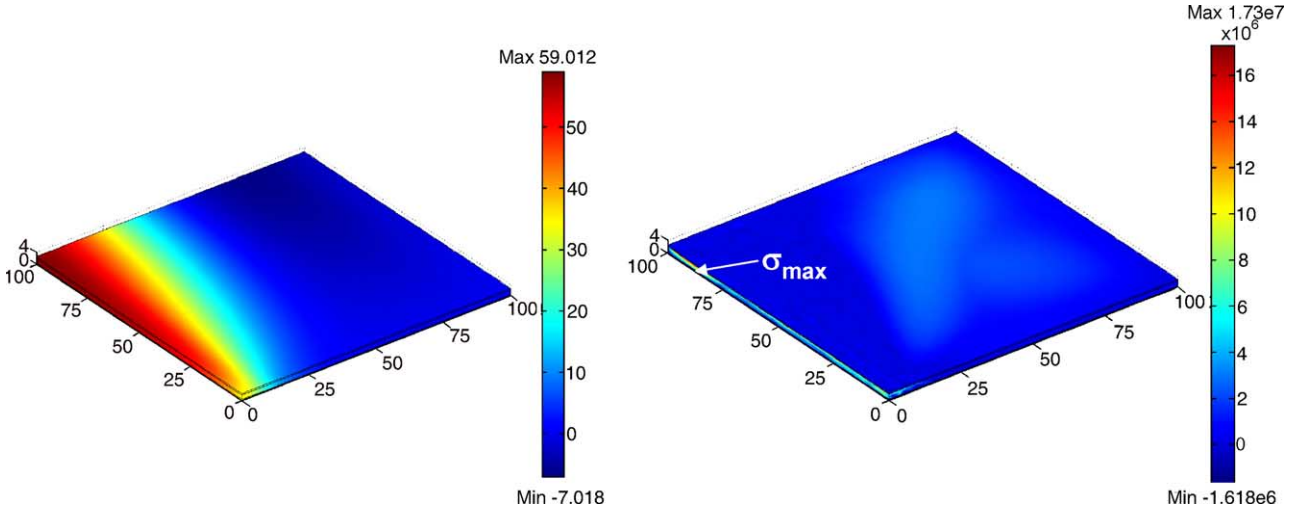

Fig. 2. Temperature gradients (left) and maximum principal stress distributions (right) of the base case.

the base case at steady state. The case results in significant temperature gradient in solid cell material of 12 °C mm^{-1} and with corresponding maximum principal stress of 17 MPa located in the electrolyte close to the interface with the anode layer and close to the fuel inlet. The location of the highest stress can be explained by the steep temperature drop caused by endothermic reforming and also by larger difference in TEC between anode and electrolyte material.

The stress exceeds the material strength of the electrolyte according to [17] (see Table 1) for probability of failure 10^{-6} but is well below the strength for probability of failure 10^{-5}. Simulations of the base case performed with the co-and counter-flow gas configurations (Fig. 3) show that the stress is moderate and below the critical when applying co-flow but increases above the limit with counter-flow comparing to the cross-flow configuration. However, the configurations with gases in counter-flow will result in the best electrical performance as given in Table 2.

If humidified hydrogen is used as fuel gas i.e. if internal reforming of methane is avoided the temperature gradients become much lower which results in maximum stresses far below the allowed limit (Fig. 3).

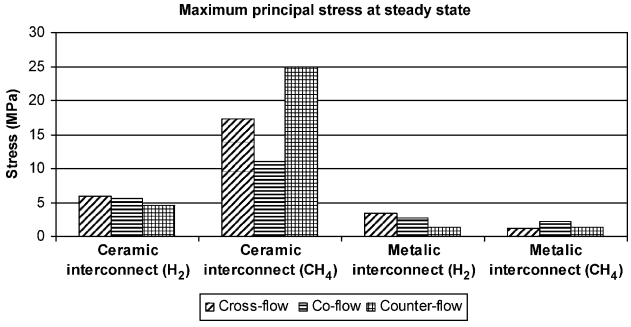

Fig. 3. Maximum principal stress of investigated cases.

When the ceramic interconnect material was replaced by metallic the stresses were lowered noticeably. This is also shown in Fig. 3. The highest stress was observed for the cell fuelled with hydrogen and with the gases in cross-flow. This was an opposite behavior if compared to the ceramic cell which experienced highest stress with reformate fuel. The decreased sensitivity to the variation of fuel and the flow type can be explained by high thermal conductivity of the metallic interconnect.

Table 2
Performance results for investigated steady state cases

Case		Electric efficiency (%)	Power density (W cm^{-2})	Air flow (mol h^{-1})
Ceramic IC, H_2 fuel	Cross-flow	39.00	0.208	18.6
	Co-flow	48.41	0.219	12.0
	Counter-flow	48.44	0.219	13.0
Ceramic IC, CH_4 fuel	Cross-flow	53.29	0.166	10.6
	Co-flow	54.20	0.152	5.1
	Counter-flow	55.95	0.157	7.2
Metallic IC, H_2 fuel	Cross-flow	49.70	0.221	12.0
	Co-flow	49.82	0.222	11.7
	Counter-flow	50.24	0.227	11.8
Metallic IC, CH_4 fuel	Cross-flow	54.06	0.214	7.0
	Co-flow	53.89	0.214	7.0
	Counter-flow	54.66	0.217	7.5

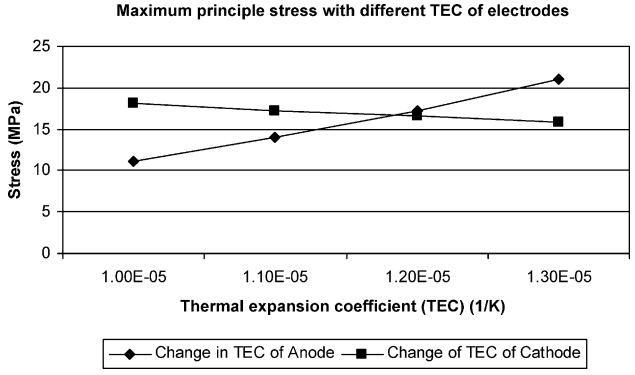

Fig. 4. Maximum principle stress at variable thermal expansion coefficient of anode and cathode layer.

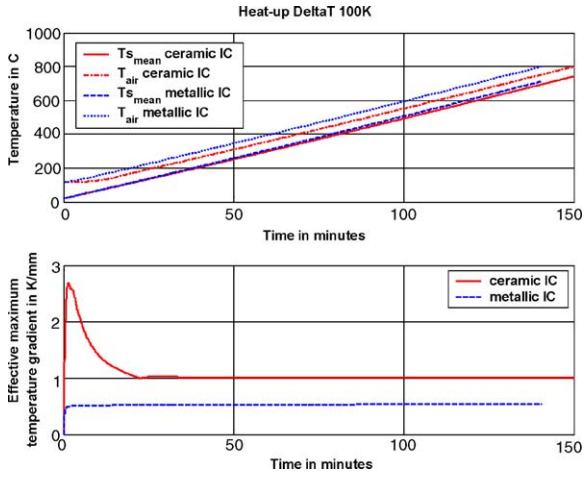

Fig. 6. Heat-up process for ΔT of 100 K.

The results of reducing the differences in TECs of the anode and cathode in respect to that of the YSZ electrolyte are shown in Fig. 4 for the base case. For fixed TEC of the electrolyte, the thermal expansion coefficients of the anode or the cathode material have been varied one at a time. By fixing the cathodic TEC and decreasing the TEC of the anode the maximum stress in the cell decreases while the opposite behavior is obtained when varying the cathodic TEC for fixed anodic TEC.

Fig. 5 shows the maximum stress variation with operating voltage and fuel utilization for the base case cell (reformate fuel, cross-flow). The maximum stress varies exponentially with the cell voltage. Operation at lower cell voltages causes higher stresses due to much higher local currents and consequently higher temperature gradients. There is a linear dependency of the maximum stress with the utilization and higher stresses can be expected with operation at lower fuel utilizations. The reason is that the heat generation at the fuel inlet decreases (due to lower currents) and the endothermic temperature drop becomes larger which causes, again, larger temperature gradients.

4.2. Dynamic heat-up

Fig. 6 presents the results of the heat-up process for cell with a cross-flow gas arrangement. A comparison has been made between the ceramic and metallic IC cell. The difference between the minimum cell temperature and the one of the incoming air, ΔT, is 100 K. While both cells need about the same time to reach the start-up temperature level of 700 °C, the trends of the maximum thermal gradients within the cells are quite different. Due to the relatively small heat conduction coefficient of the ceramic IC, higher maximum thermal gradients occur at the beginning of the heat-up process. Those thermal gradients produce a principal stress peak of 12 MPa in the cell with ceramic IC. After 30 min the principal stress decreases to a steady value of 1.9 MPa. Since the cell with metallic IC has a relatively high heat conduction coefficient, the maximum thermal gradient distribution over the time is uniform causing a continuous principal stress level of 0.9 MPa.

In Fig. 7, the results of dynamic heat-up simulations with different ΔT are presented. For increased ΔT the time needed for reaching the start-up level decreases. At the same time, the maximum principal stresses increase linearly.

4.3. Dynamic start-up

Fig. 8 presents the start-up process for a cell with ceramic IC and cross-flow gas configuration. A comparison between

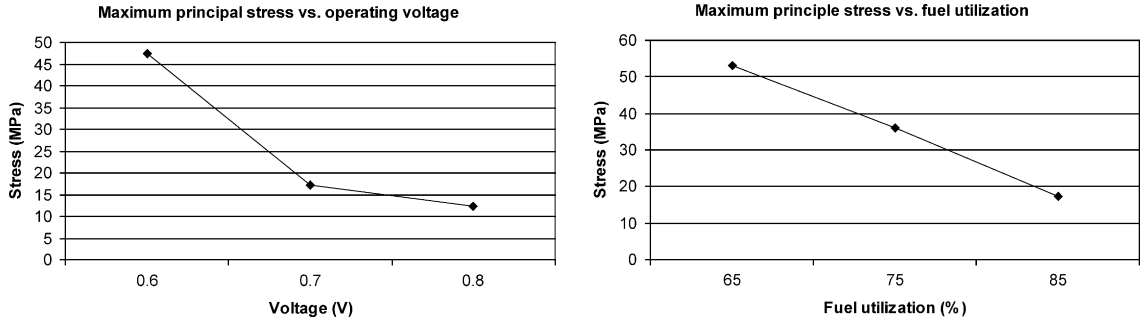

Fig. 5. Maximum principle stress variation with operating cell voltage (left) and fuel utilization (right).

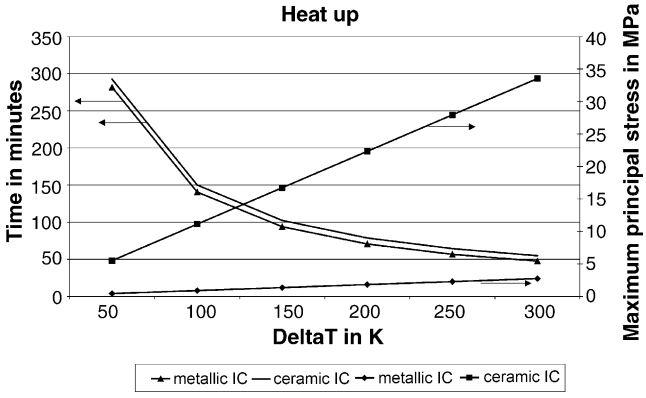

Fig. 7. Maximum principal stress and response time for the heat-up simulation at different ΔT.

the start-up of a cell operated with H_2 and one operated with CH_4 has been made.

The start-up process for the cell fed with CH_4 takes about an hour. The highest principal stress (17 MPa) occurs when steady state is reached, as already discussed. For the cell fed with H_2 the start-up process takes about 30 min. A principal stress peak of 13 MPa occurs at the beginning of the process but is still lower than the stresses occurring in the CH_4-fed cell at steady state.

The temperature profile within the cell fed with H_2 changes considerably due to heat generation by electrochemical reactions. Fig. 9 presents temperature profiles developing at different times during start-up. Since the incoming air stream at the beginning of the process heats the cell up, the maximum cell temperature can be found at the air-inlet side. At steady state, chemical reactions cause a maximum temperature of 1050 °C. However, the incoming air has a cooling effect on the cell resulting in a non-uniform temperature distribution with a maximum situated at the air-outlet/fuel-inlet corner.

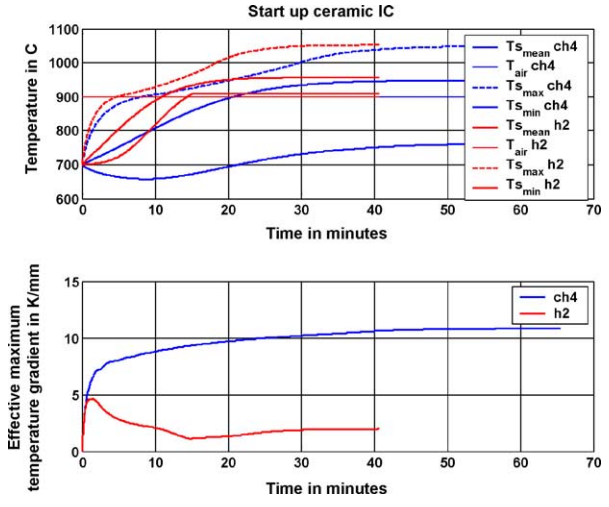

Fig. 8. Start up process for cells with ceramic IC.

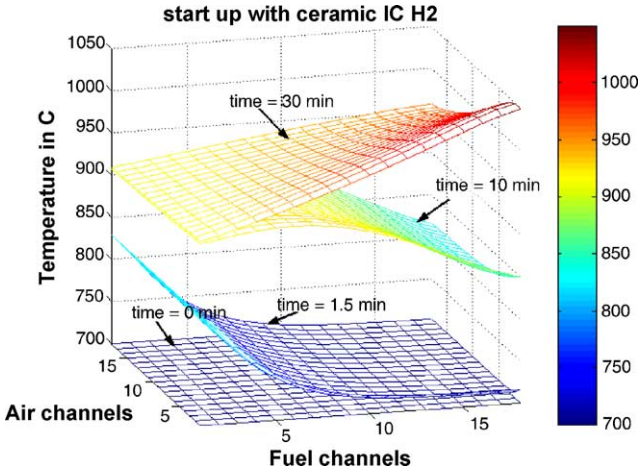

Fig. 9. Temperature profiles occurring at different times during start up of a H_2 fed cell with ceramic IC and cross-flow gas configuration.

4.4. Dynamic shut-down

The shut-down behavior of the four cases described above for a ΔT of 100 K was investigated. Similar to the heat-up process, the shut-down times for the different cell types vary not very much.

The shut-down behavior of the four cases described in Chapter 3 for a ΔT of 100 K was investigated. Similar to the heat-up process, the shut-down times for the different cell types vary not very much. Time needed to cool the cells down is about 4 h. Due to the ΔT of 100 K, the stresses do not overstep the maximum principal stresses occurring at steady state.

5. Conclusions

Capability of performing steady state and transient thermal stress analysis in a planar bipolar solid oxide fuel cell has been developed by coupling electrochemical, thermal and structural modeling. The main objective is enabling prediction of the reliability of the cell structure under given operational conditions when fuel cell is operating within a system. The modeling approach can be used in system studies but also as a simplified engineering tool in fuel cell design development. Steady state and transient stress analysis performed with different interconnect materials and different fuels showed that:

- Largest stress occurs in a ceramic cell fuelled with prereformed methane and it is located in the electrolyte layer at interface with the anode. The stress is slightly above the strength of the electrolyte material. Arranging the gases in different flow configurations can improve the cell performance but on the other hand can have a significant effect on the structural reliability of the cell.

- Introduction of the metallic interconnect can improve the temperature field of the cell and consequently lower the thermal stresses. Due to high thermal conductivity of the interconnect material the sensitivity to the choice of the fuel and flow configurations decreases which may leave more degree of freedom for system operation and design.
- Operation at lower cell voltages and lower fuel utilization may cause structural problems in planar cells.
- Comparing the heat-up process of the two different cell types of the cross flow gas arrangement shows that both cell types need about the same time to reach start-up temperature. Heating up the cells with a ΔT of 100 K takes about 2.5 h. The stresses occurring in both cells are lying beyond the limit.
- The cell with ceramic IC can be started up within about 30 min when fed with H_2 and a principal stress peak arises at the beginning of the process. Choosing CH_4 as inlet fuel, start-up takes about 1 h. Principal stress occurring within the cell is higher for the CH_4-fed cell than for the H_2-fed one.
- Shut-down with a ΔT of 100 K takes, for all investigated cases, about 4 h. The maximum principle stresses are similar to the one occurring at steady state.

For the future, continued improvement of the finite element analysis will account for the residual stresses caused by the manufacturing as well as the impact of TEC of the IC layers on the stress distribution in the single cell.

Acknowledgements

Swedish Energy Administration and Sydkraft utility are greatly acknowledged for funding this work.

References

[1] E. Ivers-Tiffe, A. Weber, D. Herbstritt, J. Eur. Ceram. Soc. 21 (2001) 1805–1811.
[2] A. Selcuk, A. Atkinson, J. Eur. Ceram. Soc. 17 (1997) 1523–1532.
[3] Structural Limitations in the Scale-up of Anode Supported SOFCs, Final report to DOE NETL, TIAX, LLC, October 2002.
[4] E. Achenbach, SOFC stack modelling, IEA report, 1996.
[5] A. Selcuk, G. Merere, A. Atkinson, J. Mater. Sci. 36 (2001) 1173–1182.
[6] P.G. Debendetti, C.G. Vayenas, Chem. Eng. Sci. 38 (11) (1983) 1817–1829.
[7] S. Ahmed, C. McPheeters, R. Kumar, J. Electrochem. Soc. 138 (9) (1991) 2712–2718.
[8] K. Nisancioglu, H. Karoliussen, R. Odegard, First European Solid Oxide Fuel Cell Forum, Luzerne, Switzerland, 1994.
[9] E. Achenbach, J. Power Sources 49 (1994) 333–348.
[10] J.R. Ferguson, J.M. Fiard, R. Herbin, J. Power Sources 58 (1996) 109–122.
[11] P. Costamagna, Electrochem. Soc. Proc. 145 (11) (1998) 3995–4007.
[12] H. Yakabe, T. Ogiwara, I. Yasuda, M. Hishinuma, Model and Stress Calculation of Planar SOFC, in: International Fuel Cell Conference, Nagoya, Japan, November/December, 1999.
[13] A. Selimovic, Modelling of Solid Oxide Fuel Cells Applied to the Analysis Of Integrated Systems with Gas Turbines, Doctoral Thesis, Lund Institute of Technology, ISRN LUTMDN/TMHP-02/1002-SE; 0282-1990 (2002).
[14] E. Achenbach, SOFC Stack Modelling, IEA Program on R,D&D on Advanced Fuel Cells, Final Report of Activity A2, Report of Research Center Julich, March 1996.
[15] C. Haynes, J. Power Sources 109 (2002) 365–376.
[16] FEMLAB 3, Structural Mechanics Module User's Guide, Comsole AB, January 2004.
[17] C.S. Montross, H. Yokokawa, M. Dokiya, Br. Ceram. Trans. 101 (3) (2000) 85–93.
[18] J. Palsson, A. Selimovic, P. Hendriksen, Intermediate Temperature SOFC in Gas Turbine Cycles, paper No 2001-GT-0091, ASME Turbo Expo 2001, New Orleans, LU, USA, June 2001.
[19] N.Q. Minh, T. Takahashi, Science and Technology of Ceramic Fuel Cells, Elsevier, 1995.